

Characterization of Intracellular Ca^{2+} Transient by the Hybrid Logistic Function in Aequorin-Injected Rabbit and Mouse Papillary Muscles

Ju MIZUNO^{1,2,3}, Mikiya OTSUJI¹, Hideko ARITA¹, Kazuo HANAOKA¹,
Shigeho MORITA², Robert AKINS³, Shuta HIRANO⁴, Yoichiro KUSAKARI⁴, and
Satoshi KURIHARA⁴

¹Department of Anesthesiology, Faculty of Medicine, The University of Tokyo, Tokyo 113-8655, Japan; ²Department of Anesthesiology, Teikyo University School of Medicine, Tokyo, 173-8605 Japan; ³Nemours Biomedical Research, and Nemours Cardiac Center, Alfred I. duPont Hospital for Children, Wilmington, DE 19803, USA; and ⁴Department of Cell Physiology, The Jikei University School of Medicine, Tokyo, 105-8461 Japan

Abstract: Myocardial intracellular calcium (Ca^{2+}) transients (CaTs) regulate tension generation and relaxation. Isometric tension curves are often analyzed using exponential equations; however, we previously demonstrated that hybrid logistic (HL) functions, which describe the difference between two S-shaped logistic functions, provide more accurate representations. In the present study, we investigated the potential application of HL functions for analyzing CaTs directly. CaTs were measured using the calcium-sensitive bioluminescent protein, aequorin, in 7 isolated rabbit right ventricular and 15 isolated mouse left ventricular papillary muscles. CaT data were fit by the least-squares method using HL and polynomial exponential (PE) function equations. The mean correlation coefficient (r) values of HL and PE fits were 0.9934 vs. 0.9523 in rabbit and 0.9980 vs. 0.9407 in mouse, respectively. The Z transformation of r value and the adjusted coefficient of determination (r squares) were higher, and

the residual mean squares and Akaike information criterion values, which estimate goodness of fit between functions with different numbers of parameters, were lower for the HL curves than for the PE curves in both rabbit and mouse. There were significant correlations between the calculated values from the best-fit HL function curve and the primary CaT data. Thus the HL function curves more accurately described the amplitudes and time courses of CaTs in both rabbit and mouse papillary muscles. We speculate that the first logistic component curve reflects the concentration and time course of Ca^{2+} inflow into the cytoplasmic space, and that the second logistic component curve reflects the concentrations and time courses of Ca^{2+} removal from the cytoplasmic space as well as Ca^{2+} binding to troponin. This approach might provide a more robust model for studying CaTs and cardiac cycle regulation.

Key words: myocardium, calcium, curve fit, cardiac cycle, excitation-contraction coupling.

Myocardial intracellular calcium (Ca^{2+}) concentration is an important determinant of mammalian myocardial tension generation and relaxation [1]. Changes in cytoplasmic Ca^{2+} , i.e., Ca^{2+} transients (CaTs), are related to the generated tension curves [2], and the increase and decrease in cytoplasmic Ca^{2+} concentration regulate myocardial contraction and relaxation, respectively. Additionally, changes in the Ca^{2+} sensitivity of cardiac troponin (Tn) substantially influence the contractile forces by altering the actin-myosin cross-bridge (CB) interaction.

The tension waveform in the myocardium and left ventricular (LV) pressure waveform in the heart provide valuable information for evaluating myocardial and cardiac performance, including inotropism and lusitropism. In this paradigm, the myocardium and LV are viewed as non-

linear oscillators that generate tension and LV pressure over time. To maximize the amount of useful information extracted from the isometric tension and isovolumic LV pressure curve waveforms, many investigators have attempted to express the tension and LV pressure curves entirely using mathematical models, such as polynomial exponential (PE) functions [3–5], even though the contraction and relaxation phases of these curves appear to be S-shaped. We previously demonstrated that tension generated in ferret papillary muscle was better represented by the difference between two S-shaped logistic functions [6]. This hybrid logistic (HL) function has also been shown to characterize isometric twitch tension curves in the cross-circulated canine right ventricular (RV) papillary muscle [7], isometric twitch and spontaneous tension curves in

Received on Nov 5, 2007; accepted on Nov 29, 2007; released online on Dec 1, 2007; doi:10.2170/physiolsci.RP013107

Correspondence should be addressed to: Ju Mizuno, Department of Anesthesiology, Teikyo University School of Medicine, 2-11-1 Kaga, Itabashi-ku, Tokyo 173-8605, Japan. Tel: +81-3-3964-2575, Fax: +81-3-3963-2687, E-mail: mizuno_ju4@yahoo.co.jp

the guinea pig ileal and colonic smooth muscles [8], and isovolumic LV pressure curves in the excised, cross-circulated canine heart [9, 10].

Since CaTs are expected to run in parallel with the time courses of tension and LV pressure curves, and since the rising and falling phases of CaTs are also presented as S-shaped curves, we investigated the potential application of HL functions for analyzing CaTs and sought to determine whether HL functions fit CaTs more precisely than standard exponential functions. Improved curve fitting using the best-fit HL function for CaTs would provide superior physiological representations of Ca^{2+} handling in cardiomyocytes. We hypothesized that the first and second logistic component curves of the best-fit HL function reflect the time courses of Ca^{2+} inflow into the cytoplasmic space and Ca^{2+} removal from the cytoplasmic space during myocardial Ca^{2+} handling, respectively.

METHODS

This study protocol was approved by the Animal Investigation Committee of the Jikei University School of Medicine. All procedures were conducted in conformity with the Guiding Principles for the Care and Use of Animals in the Field of Physiological Sciences endorsed by the American Physiological Society and the Physiological Society of Japan.

Surgical preparation. Seven albino rabbits (Japan White, body weight 2.0–2.5 kg) and 15 mice (C57BL/6, body weight 25–30 g) were anesthetized with intravenous pentobarbital sodium (1.5–2.0 mg/kg for rabbits and 15–20 mg/kg for mice). After the heart was removed, the aorta was cannulated with a blunted 18 G needle, and the heart was mounted on a Langendorff apparatus. The coronary blood was washed out with Tyrode's solution with 2 mM Ca^{2+} buffered by *N*-2-hydroxyethyl-piperazine-*N*-2-ethanesulfonic acid (HEPES) at constant pressure for 5 min. The solution was changed to HEPES-buffered Tyrode's solution containing 2 mM Ca^{2+} and 20 mM 2,3-butanedione monoxime (BDM) after the heart beat was stabilized. Once the contraction stopped completely, the heart was removed from the Langendorff apparatus. A thin papillary muscle was dissected out from the rabbit RV and mouse LV.

After both ends of the muscle were tied with silk threads, the muscle was mounted horizontally in an experimental chamber, immersed in a bath, and continuously perfused with Tyrode's solution. One end was connected to the fixed hook, and the other was attached to the arm of a tension transducer (BG-10, Kulite Semiconductor Products, Leonia, NJ; compliance 2.5 $\mu\text{m/g}$, unloaded resonant frequency 0.6 kHz). A pair of platinum black electrodes was placed parallel to the muscle, which was regularly stimulated by a single square pulse of 5 ms duration at 0.5 Hz; the strength of the stimulation was 1.5 times the

threshold. The muscle was slowly stretched and adjusted to the length at which the developed tension reached maximum (L_{max}).

The diameters of the isolated muscle specimens in the 7 rabbits and 15 mice were 0.73 ± 0.13 and 0.63 ± 0.11 mm, respectively. The muscle lengths of each rabbit and mouse were 3.30 ± 0.77 and 2.01 ± 0.43 mm, respectively.

Aequorin injection. Aequorin was dissolved in 150 mM KCl and 5 mM HEPES at pH 7.0 at a final concentration of 50–100 μM . Using glass micropipettes with a resistance of 30–50 M Ω , we pressure injected aequorin into 150–200 superficial cells of the preparation using nitrogen gas. Aequorin light signals were detected using a photomultiplier (EMI 9789A, Ruislip, UK) placed just above the muscle [11]. In twitch response, the aequorin light signal was recorded through a 500-Hz low-pass filter. Aequorin light signals were converted to cytoplasmic Ca^{2+} concentration using an *in vitro* calibration curve [12–14]. Sixty-four aequorin light signals were averaged to improve the signal-to-noise ratio. Ca^{2+} signals were sampled at 1 ms intervals and digitized with an A/D converter. All Ca^{2+} data were stored on tape (NFR-3515W, Sony Magnescale, Tokyo, Japan) and a computer (PC-9801, NEC, Tokyo, Japan) for later analysis.

Tyrode's solution. Tyrode's solution buffered with HEPES was used during all experiments, including muscle dissection and aequorin injection. The composition of the solution (in mM) was as follows: NaCl, 136.9; KCl, 5.4; MgCl_2 , 0.5; NaH_2PO_4 , 0.33; HEPES, 5; and glucose 5. The pH was adjusted to 7.40 ± 0.05 with NaOH at 24°C and equilibrated with 100% O_2 . The temperature of the solution was continuously monitored with a thermocouple and maintained at $30 \pm 0.5^\circ\text{C}$.

Calcium transient. Ca^{2+} signals were measured for 500 ms from the beginning of the twitch stimulation in both rabbit and mouse; Ca^{2+} signal returned to the resting Ca^{2+} concentration, i.e., nearly 0 $\mu\text{mol/l}$, within the 500-ms sampling window. The observed peak Ca^{2+} concentration and the time from the beginning of the twitch stimulation to the peak of CaT were measured.

The first-time derivative of Ca^{2+} concentration ($d\text{Ca}/dt$) was obtained by differentiating the sampled Ca^{2+} data after digital smoothing using an 11-point, nonweighted moving average of digitized Ca^{2+} data signals. The observed maximum of $d\text{Ca}/dt$ ($d\text{Ca}/dt_{\text{max}}$) and minimum of $d\text{Ca}/dt$ ($d\text{Ca}/dt_{\text{min}}$), the time from the beginning of the twitch stimulation to the point corresponding to $d\text{Ca}/dt_{\text{max}}$, the time from the beginning of the twitch stimulation to the point corresponding to $d\text{Ca}/dt_{\text{min}}$, the Ca^{2+} concentration at $d\text{Ca}/dt_{\text{max}}$, and the Ca^{2+} concentration at $d\text{Ca}/dt_{\text{min}}$ were measured.

Hybrid logistic equation. The following HL function [6–10], expressed as the difference between two S-shaped logistic functions, was used to fit CaT data by the least-squares method in DeltaGraph 4.0 (DeltaPoint, Monterey,

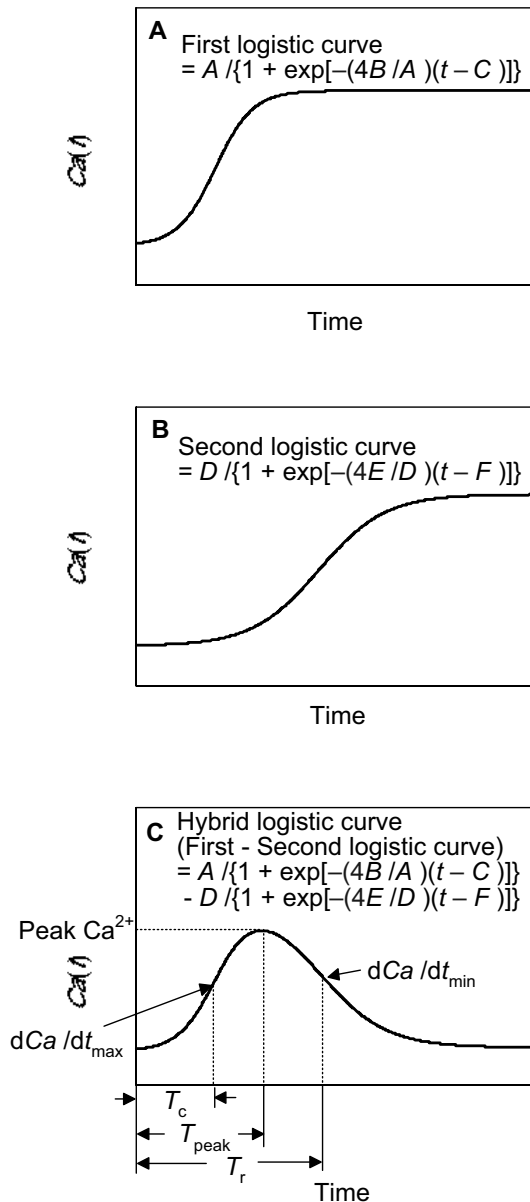


Fig 1. Hybrid logistic (HL) function. **A:** First logistic component curve. **B:** Second logistic component curve. **C:** HL function curve expressed as the difference between the first and second logistic component curves. dCa/dt_{\max} = maximum value of the first-time derivative of Ca²⁺ concentration. dCa/dt_{\min} = minimum value of the first-time derivative of Ca²⁺ concentration. T_c = time from the beginning of twitch stimulation to dCa/dt_{\max} . T_{peak} = time from the beginning of twitch stimulation to peak Ca²⁺ concentration. T_r = time from the beginning of twitch stimulation to dCa/dt_{\min} .

CA), as shown in Fig. 1:

$$Ca(t) = A / \{1 + \exp[-(4B/A)(t - C)]\} - D / \{1 + \exp[-(4E/D)(t - F)]\} + G \quad (1)$$

where t is the time from the beginning of the twitch stimulation. A is the asymptote at high t , B is the slope at the inflection point, and C is the time from the beginning of the

twitch stimulation to the inflection point of the first logistic component curve as shown in Fig. 1A. Similarly, D is the asymptote at high t , E is the slope at the inflection point, and F is the time from the beginning of the twitch stimulation to the inflection point of the second logistic component curve, as shown in Fig. 1B. G is the constant to adjust the asymptote at low t of the first logistic component curve.

Polynomial exponential equation. The following PE function [4, 5] was also used to fit CaT data by the least-squares method in DeltaGraph 4.0 (DeltaPoint, Monterey, CA),

$$Ca(t) = J (t/H)^I \exp[1 - (t/H)^I] + K \quad (2)$$

where H , I , and J are the coefficients, and K is the constant. When t arrives at H , $Ca(t)$ represents the local maximum, resulting in J plus K . I reflects the balance of the rising and falling phases.

Calculated parameters. The calculated time from the beginning of the twitch stimulation to peak Ca²⁺ concentration (T_{peak}) was obtained at the time when $dCa/dt = 0$. The calculated peak Ca²⁺ concentration was obtained by substituting T_{peak} into Eqs. 1 and 2. The calculated time from the beginning of the twitch stimulation to dCa/dt_{\max} (T_c) and dCa/dt_{\min} (T_r) was obtained as the time when $d^2Ca(t)/dt^2 = 0$. The calculated dCa/dt_{\max} and dCa/dt_{\min} were obtained by substituting T_c and T_r into $dCa(t)/dt$, respectively. The calculated Ca²⁺ concentrations at dCa/dt_{\max} and dCa/dt_{\min} were obtained by substituting T_c and T_r into Eqs. 1 and 2, respectively.

Statistical analysis. Goodness of fit was evaluated with the correlation coefficient (r) and residual mean squares (RMS). Fisher's Z transformation (Z) of r [15] was calculated with the following equation:

$$Z = 1/2[\ln(1 + r) - \ln(1 - r)] \quad (3)$$

Residual values were calculated as the observed Ca²⁺ data minus the best-fit function curve value at each sampling data point. RMS was calculated as the residual sum of squares (RSS) divided by the residual degrees of freedom, which indicates the number of data points (n) analyzed minus the number of parameters (k) in the function [16, 17].

The better-fit function was selected between the HL and PE functions with the adjusted coefficient of determination, r squares, (adjusted r^2), and Akaike information criterion (AIC), which estimate goodness of fit between functions with a different number of parameters.

The adjusted r^2 value was calculated with the following equation [18].

$$\text{Adjusted } r^2 = 1 - (1 - r^2)(n - 1)/(n - k - 1) \quad (4)$$

where n is the number of sampling data points and k is the number of parameters.

The AIC value was calculated with the following equation [18, 19].

$$AIC = n \log(RSS) + 2k \quad (5)$$

where n is the number of sampling data points and k is the number of parameters.

The Z of r , adjusted r^2 , RMS, and AIC values were compared between the goodness of HL and PE fits by a paired Student's t -test. The Z of r , adjusted r^2 , RMS, and AIC values between rabbit and mouse were compared by an unpaired Student's t -test.

The observed values from the original CaT, best-fit function parameters, and calculated values from the best-fit function curve between rabbit and mouse, were compared by an unpaired Student's t -test. A simple linear regression analysis was performed between the calculated value from the best-fit function curve and the observed value from the original CaT.

Analyses were performed using Statcel (OMS, Saitama, Japan) and StatView 5.0 (SAS Institute Inc., Cary, NC) software. Values in the text were expressed as mean \pm standard deviation (SD) unless otherwise noted. A p value of < 0.05 was considered statistically significant.

RESULTS

Calcium transient measurement

Table 1 summarizes the observed values from the original CaTs in rabbit and mouse. The observed Ca^{2+} concentration at $d\text{Ca}/dt_{\max}$, peak Ca^{2+} concentration, and Ca^{2+} concentration at $d\text{Ca}/dt_{\min}$ in rabbit were significantly lower than those in mouse. The observed time to $d\text{Ca}/dt_{\max}$, time to peak Ca^{2+} concentration, and time to $d\text{Ca}/dt_{\min}$ in rabbit were significantly longer than those in mouse. The observed $d\text{Ca}/dt_{\max}$ in rabbit was significantly less positive than that in mouse, whereas the observed $d\text{Ca}/dt_{\min}$ in rabbit was significantly less negative than that in mouse.

Hybrid logistic and polynomial exponential fits

The r , Z , adjusted r^2 , RMS, and AIC values of HL and PE fits for CaTs in the 7 rabbits and 15 mice are listed in

Table 2. The HL Z and HL adjusted r^2 values were significantly higher, and the HL RMS and HL AIC values were significantly lower than the PE values in both rabbit and mouse. Therefore the goodness of HL fit for CaT was better than the goodness of PE fit.

The HL Z and HL adjusted r^2 values were significantly lower in rabbit than in mouse. Therefore the goodness of HL fit in mouse appeared better than in rabbit.

The representative best-fit HL function curves for CaT data in rabbit and mouse muscle are shown in Fig. 2, A and B, respectively. The two S-shaped logistic component curves gradually rose and saturated at almost the same level near the end of CaT. The first logistic component curve starts earlier, rolls off near the peak Ca^{2+} concentration, and thereafter becomes the upper plateau near or over its peak Ca^{2+} concentration. The second logistic component curve lags behind the first logistic component curve. The second logistic component curve starts before

Table 2. Goodness of hybrid logistic (HL) and polynomial exponential (PE) fits for calcium transient (CaT).

	HL	PE
Rabbit		
r	0.9934	0.9523
Z	$2.85 \pm 0.23^{***\dagger}$	1.86 ± 0.21
Adjusted r^2	$0.9853 \pm 0.0074^{***\dagger}$	0.9001 ± 0.0385
RMS ($\mu\text{mol/l}$) ²	$0.0008 \pm 0.0003^{\dagger}$	$0.0057 \pm 0.0017^{*}$
AIC	$-458 \pm 150^{\dagger\dagger}$	$512 \pm 153^{**}$
Mouse		
r	0.9980	0.9407
Z	$3.45 \pm 0.21^{\dagger\dagger}$	1.74 ± 0.07
Adjusted r^2	$0.9956 \pm 0.0019^{\dagger\dagger}$	0.8830 ± 0.0151
RMS ($\mu\text{mol/l}$) ²	$0.0011 \pm 0.0007^{\dagger\dagger}$	0.0281 ± 0.0131
AIC	$-406 \pm 327^{\dagger\dagger}$	1229 ± 266

The r value indicates mean after Z transformation (Z), and the Z , adjusted r^2 , RMS, and AIC values indicate mean \pm SD of fit for CaTs data in 7 rabbit RV and 15 mouse LV papillary muscles. r = correlation coefficient. Adjusted r^2 = adjusted coefficient of determination. RMS = residual mean squares. AIC = Akaike information criterion. $^{*}p < 0.001$, $^{**}p < 0.0001$ vs. mouse. $^{\dagger}p < 0.001$, $^{\dagger\dagger}p < 0.0001$ vs. PE.

Table 1. Observed values from calcium transient (CaT).

Observed value	Rabbit	Mouse
Ca^{2+} concentration at $d\text{Ca}/dt_{\max}$ ($\mu\text{mol/l}$)	$0.31 \pm 0.08^{**}$	0.82 ± 0.19
Peak Ca^{2+} concentration ($\mu\text{mol/l}$)	$0.72 \pm 0.10^{**}$	1.70 ± 0.39
Ca^{2+} concentration at $d\text{Ca}/dt_{\min}$ ($\mu\text{mol/l}$)	$0.41 \pm 0.07^{**}$	1.23 ± 0.43
Time to $d\text{Ca}/dt_{\max}$ (ms)	$65.1 \pm 2.7^{**}$	60.1 ± 1.4
Time to peak Ca^{2+} concentration (ms)	$105.4 \pm 24.2^{*}$	76.1 ± 2.1
Time to $d\text{Ca}/dt_{\min}$ (ms)	$226.6 \pm 64.5^{**}$	107.8 ± 14.7
$d\text{Ca}/dt_{\max}$ ($\mu\text{mol/l/ms}$)	$0.041 \pm 0.013^{**}$	0.120 ± 0.029
$d\text{Ca}/dt_{\min}$ ($\mu\text{mol/l/ms}$)	$-0.011 \pm 0.003^{**}$	-0.021 ± 0.005

Mean \pm SD in 7 rabbit RV and 15 mouse LV papillary muscles. $d\text{Ca}/dt_{\max}$ = observed maximum value of the first-time derivative of Ca^{2+} data. $d\text{Ca}/dt_{\min}$ = observed minimum value of the first-time derivative of Ca^{2+} data. $^{*}p < 0.001$, $^{**}p < 0.0001$ vs. mouse.

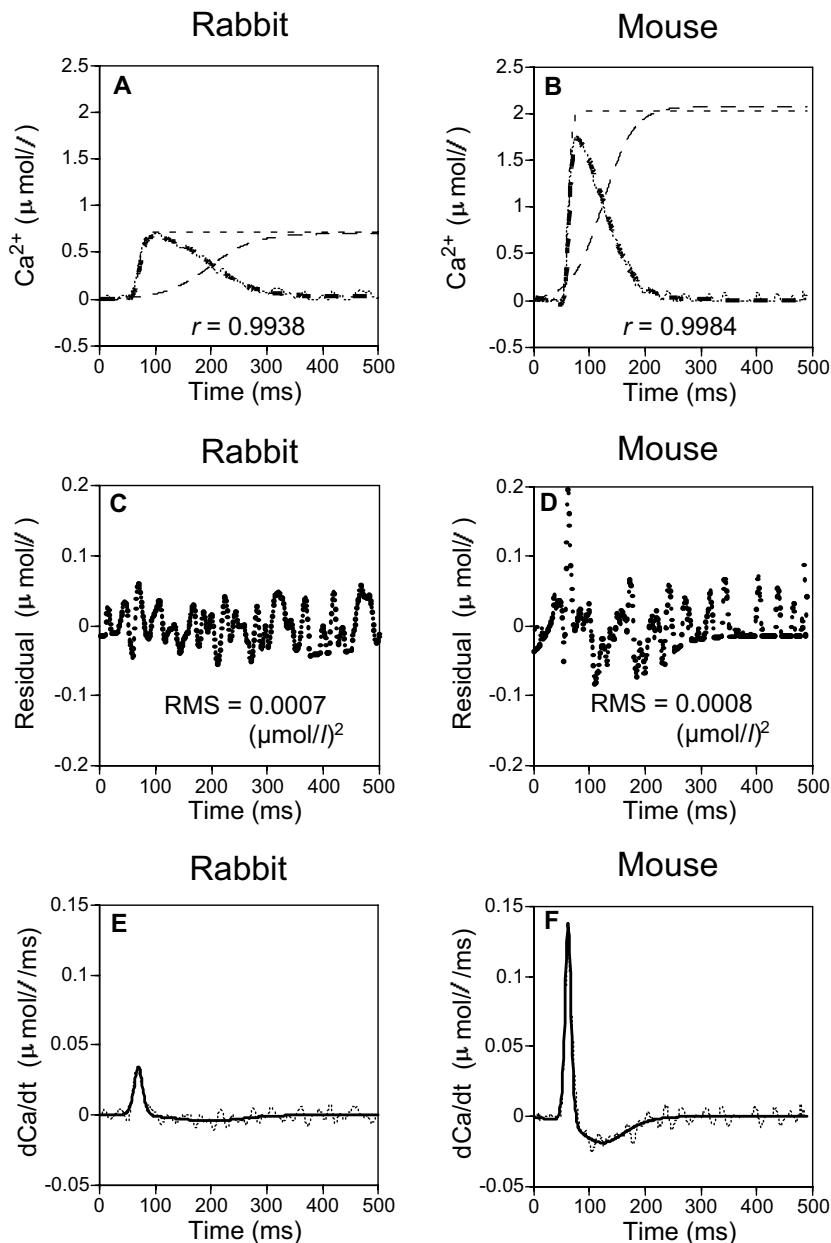


Fig 2. Representative best-fit hybrid logistic (HL) function curve for calcium transient (CaT) in a rabbit and mouse muscle. **A** and **B**: Best-fit HL function curves (thick dashed line) expressed as the difference between the first logistic (thin short-dashed line) and second logistic component curves (thin long-dashed line) for CaT data (thin dotted line) in a representative rabbit and mouse muscle, respectively. **C** and **D**: Residuals calculated as the observed Ca^{2+} data minus the calculated values from the best-fit HL function curves every 1 ms, in the same rabbit and mouse muscle as **A** and **B**, respectively. **E** and **F**: First-time derivative of the Ca^{2+} data and the calculated first-time derivative curves from the best-fit HL function curves in the same rabbit and mouse muscle as **A** and **B**, respectively.

peak Ca^{2+} concentration, rolls off, and almost reaches the plateau of the first logistic component curve near the end of CaT. The residuals, which are calculated as the differences between the original Ca^{2+} data and the calculated values from the best-fit HL function curves, in the rabbit and mouse muscles are shown in Fig. 2, C and D, respectively. The calculated first-time derivative curves from the best-fit HL function curves and the first-time derivative curves of the original Ca^{2+} data in the rabbit and mouse muscles are shown in Fig. 2, E and F, respectively.

Hybrid logistic parameters

The best-fit HL parameter A – G values for CaT in rabbit and mouse are listed in Table 3. The best-fit HL parameter A , B , D , E , and G values in rabbit were significantly lower than those in mouse. The best-fit HL parameter C and F

values in rabbit were significantly higher than those in mouse.

Calculated values from best-fit hybrid logistic function curve

The calculated values from the best-fit HL function curves in rabbit and mouse are listed in Table 4. The calculated Ca^{2+} concentrations at T_c , T_{peak} , and T_r in rabbit were significantly lower than those in mouse. The calculated T_c , T_{peak} , and T_r in rabbit were significantly longer than those in mouse. The calculated $d\text{Ca}/dt_{\text{max}}$ at T_c in rabbit was significantly less positive than that in mouse, whereas the calculated $d\text{Ca}/dt_{\text{min}}$ at T_r in rabbit was significantly less negative than that in mouse.

The relationships between the calculated values from the best-fit HL function curves and the observed values

Table 3. Best-fit hybrid logistic (HL) parameters for calcium transient (CaT).

HL parameter	Rabbit	Mouse
A ($\mu\text{mol/l}$)	$0.73 \pm 0.12^{**}$	2.04 ± 0.48
B ($\mu\text{mol/l/ms}$)	$0.047 \pm 0.021^{**}$	0.147 ± 0.037
C (ms)	$68.4 \pm 2.8^{**}$	61.4 ± 1.5
D ($\mu\text{mol/l}$)	$0.72 \pm 0.13^{**}$	2.18 ± 0.54
E ($\mu\text{mol/l/ms}$)	$0.004 \pm 0.001^{**}$	0.016 ± 0.004
F (ms)	$238.9 \pm 69.5^{**}$	117.8 ± 7.0
G ($\mu\text{mol/l}$)	$0.02 \pm 0.03^*$	0.14 ± 0.07

Mean \pm SD in 7 rabbit RV and 15 mouse LV papillary muscles. * $p < 0.001$, ** $p < 0.0001$ vs. mouse.

from the original CaT data in rabbit are shown in Fig. 3. There were significant correlations between the calculated Ca^{2+} concentration at T_{peak} and the observed peak Ca^{2+} concentration, between the calculated T_{peak} and the observed time to peak Ca^{2+} concentration, between the calculated T_r and the observed time to $d\text{Ca}/dt_{\text{min}}$, between the calculated $d\text{Ca}/dt_{\text{max}}$ at T_c and the observed $d\text{Ca}/dt_{\text{max}}$, and between the calculated $d\text{Ca}/dt_{\text{min}}$ at T_r and the observed $d\text{Ca}/dt_{\text{min}}$. However, no significant correlations were found between the calculated Ca^{2+} concentration at T_c and the observed Ca^{2+} concentration at $d\text{Ca}/dt_{\text{max}}$, between the calculated Ca^{2+} concentration at T_r and the observed Ca^{2+} concentration at $d\text{Ca}/dt_{\text{min}}$, and between the calculated T_c and the observed time to $d\text{Ca}/dt_{\text{max}}$.

The relationships between the calculated values from the HL function curves and the observed values from the original CaT data in mouse are shown in Fig. 4. Significant correlations were found between the calculated Ca^{2+} concentration at T_c and the observed Ca^{2+} concentration at $d\text{Ca}/dt_{\text{max}}$, between the calculated Ca^{2+} concentration at T_{peak} and the observed peak Ca^{2+} concentration, between the calculated Ca^{2+} concentration at T_r and the observed Ca^{2+} concentration at $d\text{Ca}/dt_{\text{min}}$, between the calculated T_c and the observed time to $d\text{Ca}/dt_{\text{max}}$, between the calculated T_{peak} and the observed time to peak Ca^{2+} concentration,

between the calculated $d\text{Ca}/dt_{\text{max}}$ at T_c and the observed $d\text{Ca}/dt_{\text{max}}$, and between the calculated $d\text{Ca}/dt_{\text{min}}$ at T_r and the observed $d\text{Ca}/dt_{\text{min}}$. However, there was no significant correlation between the calculated T_r and the observed time to $d\text{Ca}/dt_{\text{min}}$.

DISCUSSION

Our current results demonstrate that HL functions are a better fit for CaTs than PE functions in both rabbit and mouse papillary muscles. This finding strongly suggests that HL functions could be used to characterize the amplitude and time course of CaTs more accurately than PE functions could.

Hybrid logistic fit for calcium transient

Logistic functions have been widely used to express rising and falling phenomena in many fields of bioscience and to express intuitively symmetrical S-shaped curves, such as those found in mortality data [20] or growth curves [21, 22]. The logistic nature of these phenomena predicates that the process is either initially minimal, gradually increasing, then maximized to an asymptote, or initially maximal, gradually decreasing, and then minimized. Thus logistic functions are limited in their ability to represent complex functions, especially as they reach the upper or lower asymptote. HL functions are less limited and allow curve fitting to more complex sigmoid phenomena.

HL functions, which are differences between two logistic function curves, have been shown to fit precisely myocardial isometric twitch tension curves [6, 7], isometric twitch and spontaneous tension curves in smooth muscle [8], and isovolumic LV pressure curves [9, 10]. We have speculated that the first and second logistic component curves of the best-fit HL function represent increases and decreases in functional CB formation, respectively [6], and the computer simulation of Ca^{2+} and CB kinetics suggest that the cumulative CB attachment and detach-

Table 4. Calculated values from best-fit hybrid logistic (HL) function curve.

Calculated value	Rabbit	Mouse
Ca^{2+} concentration at T_c ($\mu\text{mol/l}$)	$0.34 \pm 0.05^{**}$	0.81 ± 0.18
Ca^{2+} concentration at T_{peak} ($\mu\text{mol/l}$)	$0.69 \pm 0.10^{**}$	1.66 ± 0.38
Ca^{2+} concentration at T_r ($\mu\text{mol/l}$)	$0.39 \pm 0.07^{**}$	1.09 ± 0.27
T_c (ms)	$67.4 \pm 2.8^{**}$	60.4 ± 1.5
T_{peak} (ms)	$94.4 \pm 16.7^*$	74.2 ± 2.0
T_r (ms)	$237.9 \pm 69.4^{**}$	116.8 ± 7.0
$d\text{Ca}/dt_{\text{max}}$ at T_c ($\mu\text{mol/l/ms}$)	$0.047 \pm 0.020^{**}$	0.138 ± 0.034
$d\text{Ca}/dt_{\text{min}}$ at T_r ($\mu\text{mol/l/ms}$)	$-0.004 \pm 0.001^{**}$	-0.016 ± 0.035

Mean \pm SD in 7 rabbit RV and 15 mouse LV papillary muscles. T_c = calculated time from the beginning of twitch stimulation to $d\text{Ca}/dt_{\text{max}}$. T_{peak} = calculated time from the beginning of twitch stimulation to peak Ca^{2+} concentration. T_r = calculated time from the beginning of twitch stimulation to $d\text{Ca}/dt_{\text{min}}$. $d\text{Ca}/dt_{\text{max}}$ = calculated maximum value of the first-time derivative of Ca^{2+} concentration. $d\text{Ca}/dt_{\text{min}}$ = calculated minimum value of the first-time derivative of Ca^{2+} concentration. * $p < 0.001$, ** $p < 0.0001$ vs. mouse.

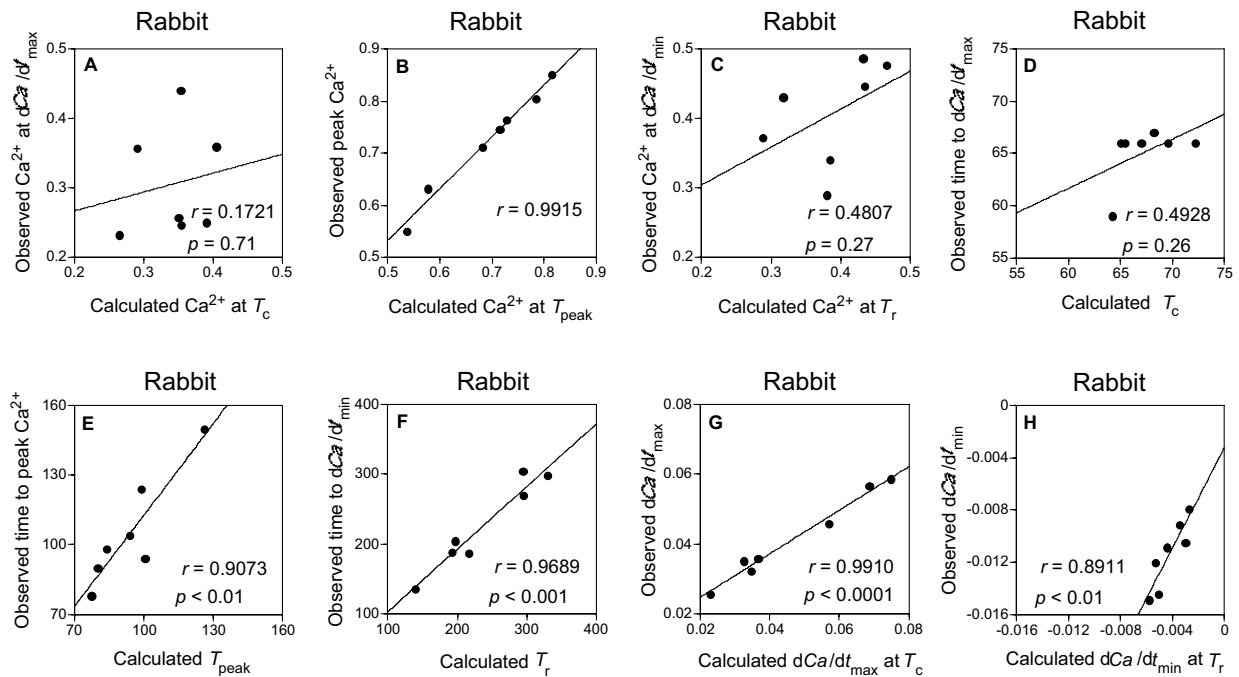


Fig. 3. Calculated values from best-fit hybrid logistic (HL) function curve and observed values from calcium transient (CaT) in seven rabbit RV papillary muscles. **A:** Relationship between the calculated Ca^{2+} concentration at T_c and the observed Ca^{2+} concentration at $d\text{Ca}/dt_{\max}$. **B:** Relationship between the calculated Ca^{2+} concentration at T_{peak} and the observed peak Ca^{2+} concentration. **C:** Relationship between the calculated Ca^{2+} concentration at T_r and the observed Ca^{2+} concentration at $d\text{Ca}/dt_{\min}$. **D:** Relationship between the calculated T_c and the

observed time from the beginning of twitch stimulation to $d\text{Ca}/dt_{\max}$. **E:** Relationship between the calculated T_{peak} and the observed time from the beginning of twitch stimulation to peak Ca^{2+} concentration. **F:** Relationship between the calculated T_r and the observed time from the beginning of twitch stimulation to $d\text{Ca}/dt_{\min}$. **G:** Relationship between the calculated $d\text{Ca}/dt_{\max}$ at T_c and the observed $d\text{Ca}/dt_{\max}$. **H:** Relationship between the calculated $d\text{Ca}/dt_{\min}$ at T_r and the observed $d\text{Ca}/dt_{\min}$. Solid line = regression line. r = correlation coefficient. p = p value.

ment curves are also logistic functions [23]. In the current study, the first logistic component curve of the HL fit for CaT data, which starts early, rolls off near the peak Ca^{2+} concentration, and thereafter becomes an upper plateau (Fig. 2), seems to represent the rising phase of CaT without the falling phase of CaT. The second logistic component curve, which lags behind the first one, starts before peak Ca^{2+} concentration, rolls off, and almost reaches the upper plateau of the first logistic component curve near the end of the falling phase of CaT, appears to mainly reflect the falling phase of CaT. This interpretation indicates that the two logistic component curves start to interact early in CaT and mainly interact until the time of peak Ca^{2+} concentration. We therefore expect that the first logistic component curve mainly reflects the time course of the Ca^{2+} inflow into the cytoplasmic space (i.e., Ca^{2+} -induced Ca^{2+} release from the sarcoplasmic reticulum [SR] triggered by Ca^{2+} influx via L-type Ca^{2+} channels in the sarcolemma). Similarly, the second logistic component curve may reflect the time course of Ca^{2+} removal from the cytoplasmic space (i.e., Ca^{2+} sequestration into SR and Ca^{2+} removal to the extracellular space). Tension and LV pressure are still being generated even as the CaT has begun to decay. In other words, the interaction between Ca^{2+}

and Tn would still be ongoing even as the Ca^{2+} signal is decaying. Therefore the falling phase of CaT may provide information about both the removal of Ca^{2+} from the cytoplasm and the interaction of Ca^{2+} with Tn. Dampening in the first logistic component curve would be associated with the decrease in Ca^{2+} inflow rate, and in the second component curve it may be associated with decreased Ca^{2+} removal and/or increased Ca^{2+} -Tn binding, which would be reflected in force data. It should also be pointed out that some investigators have expressed the falling part of CaTs from $d\text{Ca}/dt_{\min}$ to the end point using mono-exponential [24–32] and double mono-exponential functions [33, 34]. It has recently been shown, however, that the half-logistic function fits the falling phase of CaT more precisely than the mono-exponential function does [35]. Thus the half-logistic time constant (τ_l) may be superior as an index of velocity to the conventional mono-exponential time constant (τ_E) [35]. Similarly, we suppose that the half-logistic function could fit the rising phase of CaT from the beginning of twitch stimulation to $d\text{Ca}/dt_{\max}$ more precisely than the mono-exponential function. Thus it may be possible to obtain significant insight into myocardial Ca^{2+} handling under different physiological or pathological conditions by analyzing HL function coefficients.

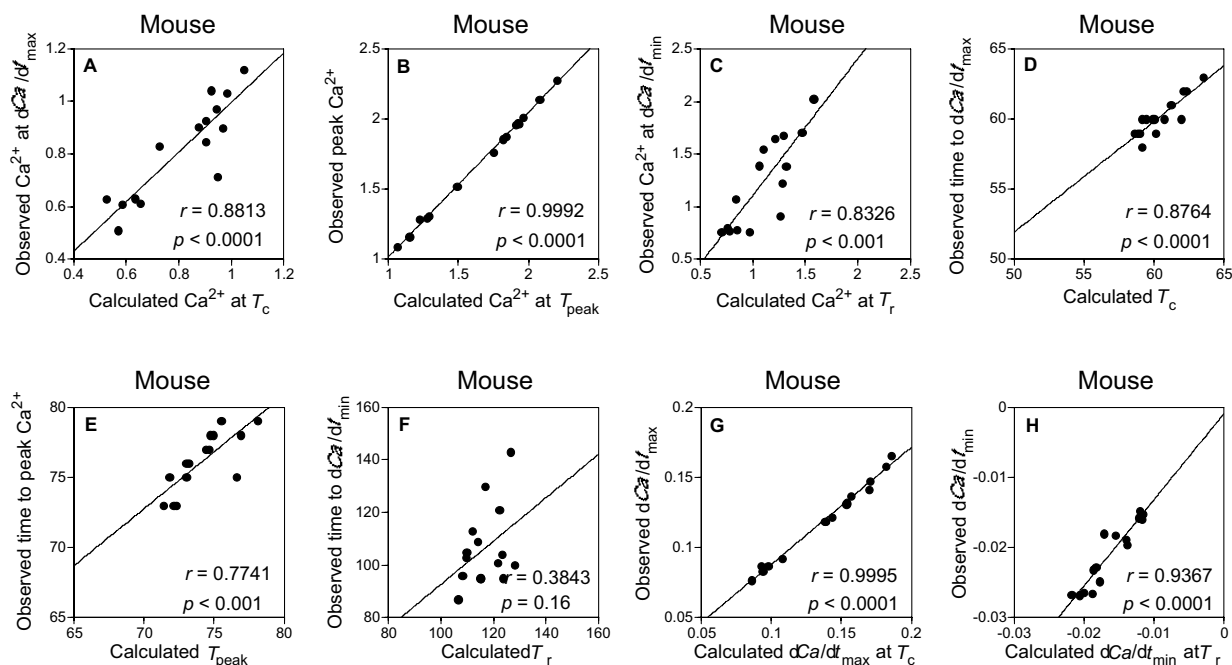


Fig 4. Calculated values from best-fit hybrid logistic (HL) function curve and observed values from calcium transient (CaT) curve in 15 mouse LV papillary muscles. **A:** Relationship between the calculated Ca^{2+} concentration at T_c and the observed Ca^{2+} concentration at $d\text{Ca}/dt_{\max}$. **B:** Relationship between the calculated Ca^{2+} concentration at T_{peak} and the observed peak Ca^{2+} concentration. **C:** Relationship between the calculated Ca^{2+} concentration at T_r and the observed Ca^{2+} concentration at $d\text{Ca}/dt_{\min}$. **D:** Relationship between the calculated T_c and the observed time from the beginning of twitch

stimulation to $d\text{Ca}/dt_{\max}$. **E:** Relationship between the calculated T_{peak} and the observed time from the beginning of twitch stimulation to peak Ca^{2+} concentration. **F:** Relationship between the calculated T_r and the observed time from the beginning of twitch stimulation to $d\text{Ca}/dt_{\min}$. **G:** Relationship between the calculated $d\text{Ca}/dt_{\max}$ at T_c and the observed $d\text{Ca}/dt_{\max}$. **H:** Relationship between the calculated $d\text{Ca}/dt_{\min}$ at T_r and the observed $d\text{Ca}/dt_{\min}$. Solid line = regression line. r = correlation coefficient. p = p value.

In using PE functions as empirical models for evaluating cardiac function, Nwasokwa suggests that three PE coefficients for tension or LV pressure curves provide physiological information [3–5]. The parameter H reflects the chronotropic state or the time from the beginning of the twitch stimulation to peak tension or LV pressure; the parameter I reflects the lusitropic state and is closely related to the ratio of the minimum of the first-time derivative of tension (dF/dt_{\min}) to the maximum of the first-time derivative of tension (dF/dt_{\max}), or the minimum of the first-time derivative of pressure (dP/dt_{\min}) to the ratio of the maximum of the first-time derivative of pressure (dP/dt_{\max}); and the parameter J reflects the inotropic state and is numerically related to peak tension or peak LV pressure. When such PE models are applied to the time courses of CaTs, the parameter J might be related to Ca^{2+} inflow into the cytoplasmic space, and the parameter I might be related to Ca^{2+} removal from the cytoplasmic space and the Ca^{2+} -Tn interaction. Since the goodness of HL fits for the isometric tension [6, 7], the isovolumic LV pressure curves [9], and the CaTs are better than the goodness of PE fits, the HL coefficients should provide a more accurate assessment of Ca^{2+} dynamics.

In the present study, one set of conditions was used to

show that HL functions precisely fit CaTs, i.e., 100% L_{\max} with 2 mM extracellular Ca^{2+} at 30°C. Isometric tension and isovolumic LV pressure curves, however, have been fit with HL functions under various physiological and pharmacological conditions. HL functions fit precisely isometric tension curves at any muscle length and at any extracellular Ca^{2+} concentration [6], or under a pharmacological inhibition of ileal contraction by nociceptin [8]. Moreover, cardiac preparations under increasing preload [9, 10] and contractility with Ca^{2+} infusion into the coronary artery [9] show the best fit using HL functions. These findings suggest that HL functions would also be applicable to CaTs under various physiological and pharmacological states.

The parameters A – F determined for HL fits for tension curves are highly correlated with the observed peak tension (F_{peak}), dF/dt_{\max} , time to dF/dt_{\max} , F_{peak} , dF/dt_{\min} , and time to dF/dt_{\min} , respectively [6–8]. The calculated values from HL fits for LV pressure curves correspond to the observed data [9]. Similarly, the parameters A – F determined for HL fits for LV pressure curves are highly correlated with the observed peak pressure (P_{peak}), dP/dt_{\max} , time to dP/dt_{\max} , P_{peak} , dP/dt_{\min} , and time to dP/dt_{\min} , respectively [9]. In the present study, some values calculated from

the best-fit HL function curve for CaT data did not correspond perfectly to the observed values, and the r values of HL fit for CaTs seem lower than those for the tension [6, 7] and LV pressure curves [9, 10]. The lower r values might be related to the accuracy of Ca²⁺ measurements using aequorin [11-13]. The main indices of CaTs, however, are predicted by the best-fit HL function curve. In particular, the calculated dCa/dt_{\max} and dCa/dt_{\min} values, which are useful indices for CaT, may present more reliable values than those determined by sampling at a rate of 1 kHz. A further examination of these concepts under different physiological, pharmacological, and pathological conditions is needed.

Species differences in calcium transient

The molecular details of Ca²⁺ handling depend on the species investigated [30]. Species differences are mainly dependent on the duration of Ca²⁺ release from the SR that is induced by Ca²⁺ influx through L-type Ca²⁺ channels [28], SR Ca²⁺-ATPase activity [29], and sodium (Na⁺)-Ca²⁺ exchanger [36]. For example, τ_E for the CaT decline curve in mouse myocytes is reported to be lower than that in rabbit myocytes [29]. We have also found that τ_L and τ_E for the CaT decline curve in mouse are smaller than those in rabbit [35]. In the mouse myocyte, the peak increase in L-type Ca²⁺ current is smaller, and the SR Ca²⁺ content, SR Ca²⁺-ATPase activity, and outward Na⁺-Ca²⁺ exchanger current are greater than in the rabbit myocyte [28, 29]. Our results show that the Ca²⁺ concentrations at T_c , T_{peak} , and T_r in mouse are higher than those in rabbit, although T_c , T_{peak} , and T_r in mouse are shorter than those in rabbit (Table 4). Therefore dCa/dt_{\max} in mouse is more positive than that in rabbit, whereas dCa/dt_{\min} in mouse is more negative than that in rabbit. These findings are consistent with substantial species differences in SR Ca²⁺-ATPase activity and Na⁺-Ca²⁺ exchanger density, which are important determinants of dCa/dt_{\min} .

The goodness of HL fit in rabbit is inferior to that in mouse. A few calculated values from the best-fit HL function curve in rabbit do not show good correlations (Fig. 3). With the exception of T_r , most calculated values from the best-fit HL function curve in mouse show excellent correlations (Fig. 4). This result may be due to the lower signal-to-noise ratio for cardiac muscle characterization in rabbit or the use of fewer rabbit muscle samples (7 rabbit vs. 15 mouse).

Conclusions

We conclude that HL functions are a better fit for CaTs than PE functions are in both rabbit RV and mouse LV papillary muscles. HL functions accurately describe the amplitudes and time courses of CaTs. We speculate that the first logistic component curve reflects the concentration and time course of Ca²⁺ inflow into the cytoplasmic space, and that the second logistic component curve re-

flects the concentrations and time courses of Ca²⁺ removal from the cytoplasmic space as well as Ca²⁺ binding to Tn. This modeling approach may provide new insight into the integration of CaTs in cardiac cycle regulation and CB dynamics.

APPENDIXES

$dCa(t)/dt$ was given from Eq. 1.

$$dCa(t)/dt = 4B/[\exp\{(2B/A)(t-C)\} + \exp\{(-2B/A)(t-C)\}]^2 - 4E/[\exp\{(2E/D)(t-F)\} + \exp\{(-2E/D)(t-F)\}]^2 \quad (6)$$

The second time derivative of Ca data ($d^2Ca(t)/dt^2$) was given from Eq. 2.

$$d^2Ca(t)/dt^2 = -(16B^2/A)[\exp\{(2B/A)(t-C)\} - \exp\{(-2B/A)(t-C)\}] / [\exp\{(2B/A)(t-C)\} + \exp\{(-2B/A)(t-C)\}]^3 + (16E^2/D)[\exp\{(2E/D)(t-F)\} - \exp\{(-2E/D)(t-F)\}] / [\exp\{(2E/D)(t-F)\} + \exp\{(-2E/D)(t-F)\}]^3 \quad (7)$$

T_{peak} was obtained as the time when $dCa(t)/dt = 0$ using Eq. 6. Peak Ca²⁺ concentration was calculated by substituting T_{peak} into Eq. 1. T_c and T_r were obtained as the time when $d^2Ca(t)/dt^2 = 0$ using Eq. 7. dCa/dt_{\max} and dCa/dt_{\min} were calculated by substituting T_c and T_r into Eq. 6, respectively. Ca²⁺ concentrations at dCa/dt_{\max} and dCa/dt_{\min} were calculated by substituting T_c and T_r into Eq. 1, respectively.

The rising phase of CaT was defined as the duration from the beginning of the twitch stimulation to peak Ca²⁺ concentration. The falling phase of CaT was defined as the duration from peak Ca²⁺ concentration to the end point.

The following logistic function was used to fit the rising and falling phases of CaT data by the least-squares method in DeltaGraph 4.0 (DeltaPoint, Monterey, CA):

$$Ca(t) = L/[1 + \exp\{-(4M/L)(t-N)\}] + O \quad (8)$$

where t is the time from the beginning of the twitch stimulation, L is the asymptote, M is the slope at the inflection point, N is the time from the beginning of the twitch stimulation to the inflection point, and O is the constant.

The following linear function was also used to fit the rising and falling phases of CaT data by the least-squares method in DeltaGraph 4.0 (DeltaPoint, Monterey, CA).

$$Ca(t) = Pt + Q \quad (9)$$

where P is the coefficient and Q is the constant.

The r , Z , adjusted r^2 , RMS, and AIC values of logistic and linear fits for the rising and falling phases of CaT data in the 7 rabbits and 15 mice are listed in Table 5. The logistic Z and logistic adjusted r^2 values were significantly higher, and the logistic RMS and logistic AIC values were

Table 5. Goodness of logistic and linear fits for rising and falling phases of calcium transient (CaT).

	Rising phase		Falling phase	
	Logistic	Linear	Logistic	Linear
Rabbit				
<i>r</i>	0.9975	0.8687	0.9922	0.9433
<i>Z</i>	$3.33 \pm 0.37^{*††}$	$1.33 \pm 0.30^{**}$	$2.77 \pm 0.21^{*††}$	$1.77 \pm 0.49^{**}$
Adjusted <i>r</i> ²	$0.9835 \pm 0.0045^{*†}$	$0.7263 \pm 0.1430^{**}$	$0.9831 \pm 0.0078^{*††}$	$0.8524 \pm 0.1093^{**}$
RMS (mol/l) ²	$0.0005 \pm 0.0002^{*††}$	$0.0213 \pm 0.0086^{**}$	$0.0008 \pm 0.0003^{†}$	$0.0090 \pm 0.0062^{*}$
AIC	$-355 \pm 115^{*††}$	$107 \pm 59^{**}$	$-440 \pm 113^{†}$	298 ± 404
Mouse				
<i>r</i>	0.9986	0.7648	0.9988	0.7692
<i>Z</i>	$3.64 \pm 0.18^{††}$	1.01 ± 0.05	$3.72 \pm 0.30^{††}$	1.02 ± 0.06
Adjusted <i>r</i> ²	$0.9969 \pm 0.0013^{††}$	0.5729 ± 0.0345	$0.9972 \pm 0.0018^{††}$	0.5797 ± 0.0359
RMS (mol/l) ²	$0.0011 \pm 0.0004^{††}$	0.1610 ± 0.06843	$0.0006 \pm 0.0005^{††}$	0.3831 ± 0.2766
AIC	$-194 \pm 35^{††}$	189 ± 36	$-686 \pm 306^{††}$	628 ± 518

The *r* value indicates the mean after *Z* transformation (*Z*), and the *Z*, adjusted-*r*², RMS, and AIC values indicate the mean \pm SD of fit for the rising or falling CaTs in 7 rabbit RV and 15 mouse LV papillary muscles. *r* = correlation coefficient. Adjusted *r*² = adjusted coefficient of determination. RMS = residual mean squares. AIC = Akaike information criterion. **p* < 0.05, ***p* < 0.001 vs. mouse. †*p* < 0.05, ††*p* < 0.001 vs. linear function.

significantly lower than the linear ones in rabbit and mouse. Therefore the goodness of logistic fit for the rising and falling phases of CaT was better than that of linear fit. This result shows the rising and falling phases of CaT as S-shaped forms and not as linear forms.

This investigation was supported in part by a Grant-in-Aid for Scientific Research from the Ministry of Education, Culture, Sports, Science and Technology, Japan, and by grants from the Japanese Private School Promotion Foundation, the Vehicle Racing Commemorative Foundation, to S. K., the Nemours Foundation and the U.S. National Center for Research Resources to R. A., and the Mochida Memorial Foundation for Medical and Pharmaceutical Research, to J. M.

REFERENCES

1. Ebashi S, Endo M. Calcium ion and muscle contraction. *Prog Biophys Mol Biol*. 1968;18:123-83.
2. Kurihara S. Regulation of cardiac muscle contraction by intracellular Ca²⁺. *Jpn J Physiol*. 1994;44:591-611.
3. Nwasokwa ON, Bodenheimer MM. Analysis of myocardial isometric dynamics using parameters of a global model. *Am J Physiol*. 1989;257:H1275-86.
4. Nwasokwa ON. Similarities and differences in the time course of mechanical activity of the canine myocardium and isovolumic left ventricle. *Jpn J Physiol*. 1996;46:327-36.
5. Nwasokwa ON. A model of the time course of myocardial dynamics: use in characterisation of relaxation and evaluation of its indices. *Cardiovasc Res*. 1993;27:1510-21.
6. Mizuno J, Mikane T, Araki J, Hatashima M, Moritan T, Ishikawa T, Komukai K, Kurihara S, Hirakawa M, Suga H. Hybrid logistic characterization of isometric twitch force curve of isolated ferret right ventricular papillary muscle. *Jpn J Physiol*. 1999;49:145-58.
7. Sakamoto T, Takaki M, Hata Y, Matsubara H, Araki J, Suga H. Hybrid logistic characterization of isometric twitch force-time curve of intact blood-perfused canine right ventricular papillary muscle. *Jpn J Physiol*. 1997;47:283-9.
8. Sugimori S, Kadowaki M, Yoneda S, Yamanouchi M, Nakano H, Takaki M. New method for evaluating intestinal contractions in guinea pig by curve fitting. *Dig Dis Sci*. 2000;45:136-44.
9. Matsubara H, Araki J, Takaki M, Nakagawa ST, Suga H. Logistic characterization of left ventricular isovolumic pressure-time curve. *Jpn J Physiol*. 1995;45:535-52.
10. Mizuno J, Shimizu J, Mohri S, Araki J, Hanaoka K, Yamada Y. Hypovolemia does not affect speed of isovolumic left ventricular contraction and relaxation in excised canine heart. *Shock*. 2007 (in press)
11. Allen DG, Kurihara S. The effects of muscle length on intracellular calcium transients in mammalian cardiac muscle. *J Physiol*. 1982;327:79-94.
12. Allen DG, Blinks JR, Prendergast FG. Aequorin luminescence: relation of light emission to calcium concentration—a calcium-independent component. *Science*. 1977;195:996-8.
13. Blinks JR, Wier WG, Hess P, Prendergast FG. Measurement of Ca²⁺ concentrations in living cells. *Prog Biophys Mol Biol*. 1982;40:1-114.
14. Okazaki O, Suda N, Hongo K, Konishi M, Kurihara S. Modulation of Ca²⁺ transients and contractile properties by beta-adrenoceptor stimulation in ferret ventricular muscles. *J Physiol*. 1990;423:221-40.
15. Snedecor GW, Cochran WG. *Statistical Methods*. 6th ed. Ames, Iowa: Iowa State Univ Press, 1971, pp185.
16. Thompson DS, Waldron CB, Coltart DJ, Jenkins BS, Webb-Peploe MM. Estimation of time constant of left ventricular relaxation. *Br Heart J*. 1983;49:250-8.
17. Thompson DS, Wilmschurst P, Juul SM, Waldron CB, Jenkins BS, Coltart DJ, Webb-Peploe MM. Pressure-derived indices of left ventricular isovolumic relaxation in patients with hypertrophic cardiomyopathy. *Br Heart J*. 1983;49:259-67.
18. Johnson JB, Ormland KS. Model selection in ecology and evolution. *Trends Ecol Evol*. 2004;19:101-8.
19. Buchwald P, Sveiczler A. The time-profile of cell growth in fission yeast: model selection criteria favoring bilinear models over exponential ones. *Theor Biol Med Model*. 2006;3:16.
20. Wilson DL. The analysis of survival (mortality) data: fitting Gompertz, Weibull, and logistic functions. *Mech Ageing Dev*. 1994;74:15-33.
21. Sheehy JE, Mitchell PL, Ferrer AB. Bi-phasic growth patterns in rice. *Ann Bot (Lond)*. 2004;94:811-7.
22. Fujikawa H, Morozumi S. Modeling Surface Growth of *Escherichia coli* on Agar Plates. *Appl Environ Microbiol*. 2005;71:7920-6.
23. Sakamoto T, Matsubara H, Hata Y, Shimizu J, Araki J, Takaki M, Suga H. Logistic character of myocardial twitch force curve: simulation. *Heart Vessels*. 1996;11:171-9.
24. Camacho SA, Brandes R, Figueredo VM, Weiner MW. Ca²⁺ transient decline and myocardial relaxation are slowed during low flow ischemia in rat hearts. *J Clin Invest*. 1994;93:951-7.
25. Chang KC, Schreier JH, Weiner MW, Camacho SA. Impaired Ca²⁺ handling is an early manifestation of pressure-overload hypertrophy in rat hearts. *Am J Physiol*. 1996;271:H228-34.
26. Halow JM, Figueredo VM, Shames DM, Camacho SA, Baker AJ. Role of slowed Ca²⁺ transient decline in slowed relaxation during myocardial ischemia. *J Mol Cell Cardiol*. 1999;31:1739-48.

27. Lim CC, Apstein CS, Colucci WS, Liao R. Impaired cell shortening and relengthening with increased pacing frequency are intrinsic to the senescent mouse cardiomyocyte. *J Mol Cell Cardiol.* 2000;32:2075-82.
28. Su Z, Sugishita K, Li F, Ritter M, Barry WH. Effects of FK506 on [Ca²⁺]_i differ in mouse and rabbit ventricular myocytes. *J Pharmacol Exp Ther.* 2003;304:334-41.
29. Su Z, Li F, Spitzer KW, Yao A, Ritter M, Barry WH. Comparison of sarcoplasmic reticulum Ca²⁺-ATPase function in human, dog, rabbit, and mouse ventricular myocytes. *J Mol Cell Cardiol.* 2003;35:761-7.
30. Bassani JW, Bassani RA, Bers DM. Relaxation in rabbit and rat cardiac cells: species-dependent differences in cellular mechanisms. *J Physiol.* 1994;476:279-93.
31. Bers DM, Berlin JR. Kinetics of [Ca]_i decline in cardiac myocytes depend on peak [Ca]_i. *Am J Physiol.* 1995;268:C271-7.
32. Brittsan AG, Ginsburg KS, Chu G, Yatani A, Wolska BM, Schmidt AG, Asahi M, MacLennan DH, Bers DM, Kranias EG. Chronic SR Ca²⁺-ATPase inhibition causes adaptive changes in cellular Ca²⁺ transport. *Circ Res.* 2003;92:769-76.
33. Diaz ME, Trafford AW, Eisner DA. The role of intracellular Ca buffers in determining the shape of the systolic Ca transient in cardiac ventricular myocytes. *Pflugers Arch.* 2001;442:96-100.
34. Capote J, Bolanos P, Schuhmeier RP, Melzer W, Caputo C. Calcium transients in developing mouse skeletal muscle fibres. *J Physiol.* 2005;564:451-64.
35. Mizuno J, Otsuji M, Takeda K, Yamada Y, Arita H, Hanaoka K, Hirano S, Kusakari Y, Kurihara S. Superior logistic model for decay of Ca²⁺ transient and isometric relaxation force curve in rabbit and mouse papillary muscles. *Int Heart J.* 2007;48:215-32.
36. Su Z, Bridge JH, Philipson KD, Spitzer KW, Barry WH. Quantitation of Na/Ca exchanger function in single ventricular myocytes. *J Mol Cell Cardiol.* 1999;31:1125-35.